COMMUNICATION

Excitonic coupling of RNA-templated merocyanine dimer studied by higher-order transient absorption spectroscopy

Received 00th January 20xx,
Accepted 00th January 20xx

DOI: 10.1039/x0xx00000x

Julia Dietzsch,[a#] Ajay Jayachandran,[b#] Stefan Mueller,[b] Claudia Höbartner[a,c*] and Tobias Brixner[b,c*]

We report the synthesis and spectroscopic analysis of RNA containing the barbituric acid merocyanine rBAM2 as a nucleobase surrogate. Incorporation into RNA strands by solid-phase synthesis leads to fluorescence enhancement compared to the free chromophore. In addition, linear absorption studies show the formation of an excitonically coupled H-type dimer in the hybridized duplex. Ultrafast third- and fifth-order transient absorption spectroscopy of this non-fluorescent dimer suggests immediate (sub-200 fs) exciton transfer and annihilation due to the proximity of the rBAM2 units.

The synthesis of molecular aggregates with a high degree of control over the formation of their molecular excitonic states plays an important role in achieving tailored photophysics. Various factors including system–bath heterogeneity,[1,2] interchromophoric separation,[3] and the extent of excitonic delocalization[4,5] all play a major role in dictating the nature of multiexcitonic states in excitonic complexes. Due to their preorganized structure, oligonucleotide scaffolds have been widely used for the precise arrangement of various chromophores[6-8] in highly controllable aggregates,[9-12] some of them showing exciton transport properties.[13-15] Recently, we reported a barbituric acid merocyanine (BAM) chromophore as nucleobase surrogate and examined its interactions and arrangements in the context of RNA, DNA, and GNA duplex environments.[16] The formation of excitonically coupled dimers raised our interest to examine the behaviour of elongated BAM chromophores and to further investigate these structures by more advanced ultrafast spectroscopic methods.

Here, we use our recently developed technique[17] of separating single- and multi-exciton dynamics in transient absorption spectroscopy by means of systematic intensity variation of the pump pulse for a better insight into excitonic coupling interactions within a merocyanine dimer in an RNA duplex and to unravel information about how the exciton dynamics evolve in this new merocyanine dimer. The rBAM2 free nucleoside (**3**, **rBAM2^{free}**), in which the polymethine

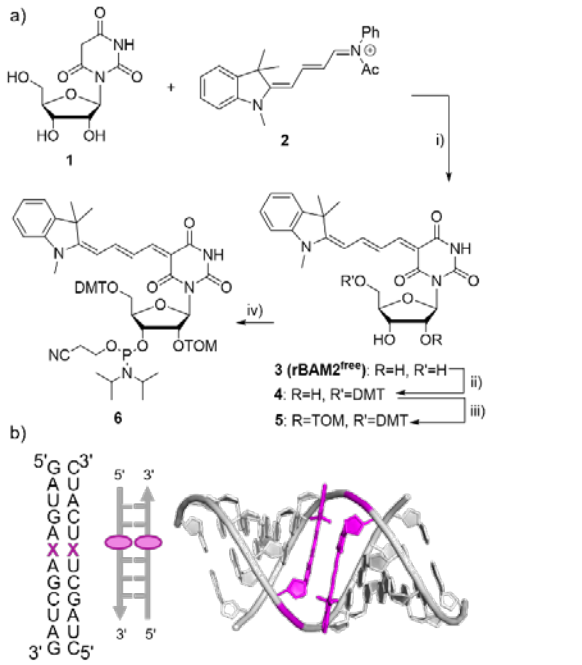

Fig. 1 (a) Reagents and conditions for the synthesis of the rBAM2 phosphoramidite building block **6**. Compounds **1** and **2** were prepared according to reported procedures.[18,19] i) NEt_3, EtOH, r. t., 30 min (76%); ii) 1. DMF-DMA, pyridine, r. t., 20 h 2. DMT-Cl, pyridine, r. t., 3 h (75%); iii) 1. DIPEA, nBu$_2$SnCl$_2$, DCE, 80 °C, 40 min. 2. TOM-Cl, r. t., 1.5 h (25%); iv) 2-cyanoethyl-*N,N*-diisopropylchlorophosphoramidite, Me_2NEt, DCM, r. t., 3 h (32%). (b) Sequence, schematic depiction and structural model of the RNA duplex studied in this work containing the rBAM2 dimer.

chain is lengthened by one vinylene unit (m(C_2H_2) = 2) compared to the previously reported rBAM (m = 1)[16] leading to a red-shift of the absorption maximum by about 100 nm,[20] was prepared by condensation of the barbituric acid β-D-ribofuranoside **1**[16] and the chromophore precursor **2**[18,19] (Fig. 1a). After installation of the 5'-*O*-DMT and 2'-*O*-TOM protecting groups, the nucleoside was converted into the target 3'-cyanoethyl phosphoramidite **6** for solid-phase RNA synthesis. To access

[a] *Institut für Organische Chemie, Universität Würzburg, Am Hubland, 97074 Würzburg, Germany*
[b] *Institut für Physikalische und Theoretische Chemie, Universität Würzburg, Am Hubland, 97074 Würzburg, Germany*
[c] *Center for Nanosystems Chemistry (CNC), Universität Würzburg, Theodor-Boveri-Weg, 97074 Würzburg, Germany*
 # These authors contributed equally.
Electronic Supplementary Information (ESI) available. See DOI: 10.1039/x0xx00000x

oligonucleotide scaffolds containing an rBAM2 opposite dimer, the 12mer RNA oligonucleotide rBAM2-S1 (5'-GAUGAXAGCUAG-3', with X = rBAM2) and its complement (5'-CUAGCUXUCAUC-3') were prepared on controlled pore glass (CPG), using compound **6** and 2'-*O*-TOM protected standard ribonucleosides. Cleavage from the solid support and removal of the base-labile protecting groups was achieved under optimized ultramild conditions by incubation of the solid support in H_2O/MeOH/NEt_3 for three days at ambient temperature. Attempts to use higher temperatures for shorter incubation time resulted in decomposition of the chromophore by nucleophilic attack onto the polymethine chain. The modified oligonucleotides were isolated by denaturing polyacrylamide gel electrophoresis, and the homogeneity and identity were confirmed by analytical anion exchange HPLC and HR-ESI-MS (see SI, Table S1).

The complementary modified oligonucleotides were mixed in equimolar ratio and annealed in phosphate buffer (pH 7.0) to form the base-paired RNA duplex rBAM2-D2 with the two rBAM2 units opposite of each other (Fig. 1b). The thermodynamic stability of the duplex was studied by thermal melting experiments, monitoring UV absorbance at 260 nm as a function of temperature (Fig. 2a). Using the baseline method,[21] a melting point of 42.1 °C was determined, which is 12.3 °C lower than an analogous unmodified RNA duplex (T_m = 54.4 °C). The melting point of the RNA duplex containing only one rBAM2 unit (rBAM2-D1, rBAM2-S1 annealed with unmodified RNA S3, 5'-CUAGCUAUCAUC-3'), was 34.1 °C. The higher thermal stability of rBAM2-D2 suggests formation of a non-covalent dimer by favourable dipolar stacking interactions in the intact duplex. This double modified duplex structure rBAM2-D2 is by ΔT = +2.9 °C more stable than the previously reported analogous duplex containing the opposite dimer of the shorter polymethine version rBAM.[16] The circular dichroism (CD) spectrum of rBAM2-D2 at ambient temperature indicated the presence of a standard A-form double helix (positive peak at 260 nm, similar to an unmodified RNA duplex), underlining that the rBAM2 dimer is accommodated in the double-stranded RNA scaffold. The CD couplet in the visible wavelength range can be attributed to exciton coupling of the interacting rBAM2 chromophores (SI, Fig. S1).

Temperature-dependent absorption spectra revealed a distinct spectroscopic behaviour of the rBAM2-D2 (Fig. 2b, blue) compared to the rBAM2 monomers in the single strands (red) present at elevated temperatures when the duplex is denatured. The transition from the dimer to the monomer spectrum takes place between 40 and 50 °C, consistent with the duplex melting temperature of 42.1 °C. The high-temperature spectrum also resembles the absorption spectrum of the free chromophore rBAM2^{free}. At 10 °C, the two chromophores exhibit pronounced exciton coupling, implied by the sharp maximum absorption peak at 516 nm which is hypsochromically shifted by 47 nm compared to the monomer absorption at 563 nm at 90 °C. The dimer spectrum also exhibits a shoulder at shorter wavelength (485 nm) and a blue-shifted second band with about 20% of the maximum intensity. These features are in agreement with the formation of an H-type aggregate.[22]

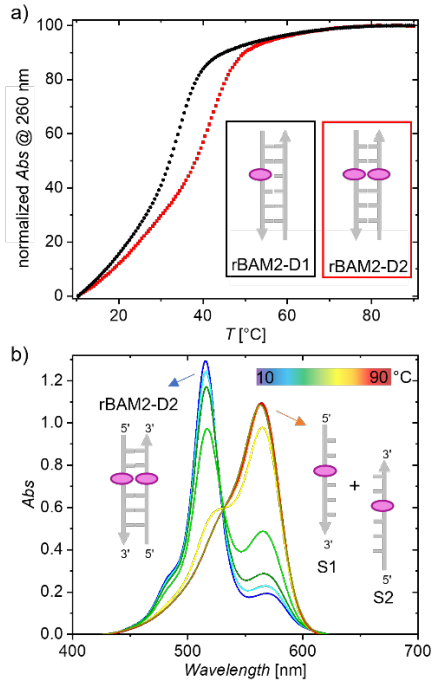

Fig. 2 (a) Thermal melting analysis of RNA duplexes containing a single rBAM2 modification (black) or an rBAM2 opposite dimer (red). (b) Temperature-dependent absorption spectra from 10 °C to 90 °C in 10 °C intervals of rBAM2-D2 indicating the formation of an H-type dimer at low temperature and monomer absorption upon denaturation into single strands.

RNA oligonucleotides containing rBAM2 showed fluorescence emission at 585 nm with increased intensity and enhanced lifetime compared to rBAM2^{free} due to rigidification of the chromophore and thereby suppressed non-radiative decay pathways (SI, Fig. S2, S3, Table S2). The highest intensity (300-fold higher than rBAM^{free}) and longest lifetime was observed for the single-modified duplex rBAM2-D1 (2.3 ns compared to <100 ps for rBAM^{free}). The intensity for the more flexible single strand rBAM2-S1 was reduced by about three times compared to the duplex rBAM2-D1 at 25 °C. Thus, melting of the duplex could also be observed by temperature-dependent emission spectra (SI, Fig S2c). The dimer-duplex rBAM2-D2 showed further reduced emission intensity (circa half of the single strand rBAM2-S1, and a factor of six lower than rBAM2-D1 at 25 °C). Interestingly, these emission spectra changed in intensity but not in spectral shape (SI, Fig. S2d). This observation is in contrast to the reported shorter rBAM chromophore, which assembled into a stacked dimer with a second emission band of lower energy and circularly polarized emission.[16] Both single strand rBAM2-S1 and dimer duplex rBAM2-D2 exhibited shorter lifetimes (1.1 and 1.7 ns) than rBAM2-D1 (SI, Fig. S3), but still longer than any of the previously investigated BAM-containing oligonucleotides.[16] The reduced intensity and shorter lifetime of rBAM2-D2 indicates fluorescence quenching by excitonic coupling due to H-aggregate formation.[13-15]

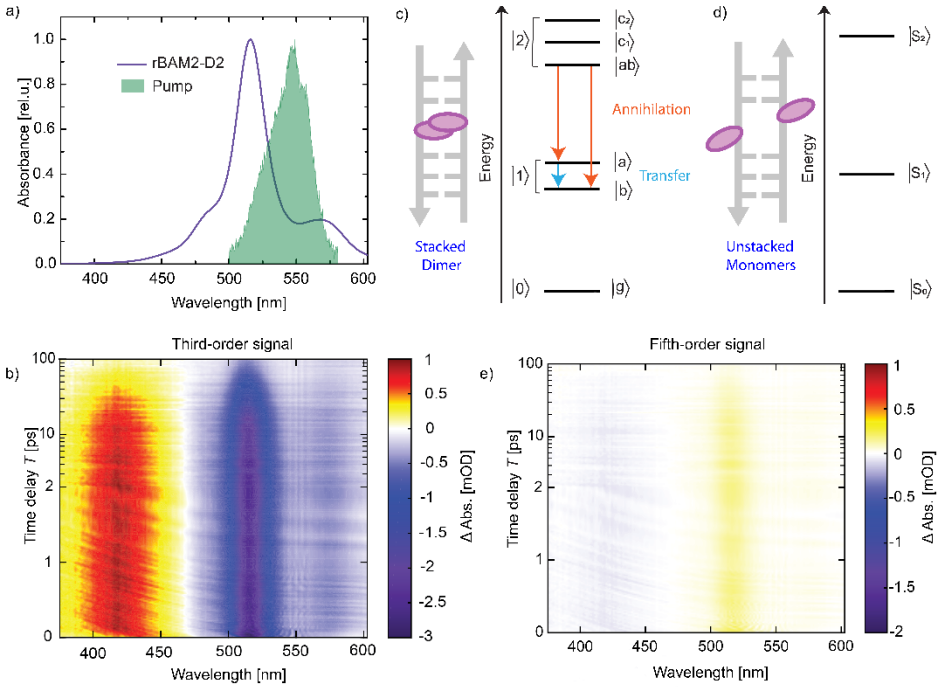

Fig. 3 (a) Linear absorption spectrum of rBAM2-D2 (purple), shown with an overlay of the spectrum of the pump pulse (shaded green area). (b) Transient absorption map of rBAM2-D2 showing the pure third-order signal. (c) Schematic depiction and energy level scheme of the rBAM2 dimer in the exciton basis with a doubly excited manifold $|2\rangle$ constituting the higher excited states $|c_1\rangle$ and $|c_2\rangle$ along with a biexciton state $|ab\rangle$. The orange arrows indicate annihilation from the biexciton state to the single-exciton manifold $|1\rangle$ constituting the single-exciton states $|a\rangle$ and $|b\rangle$ while the light blue arrow indicates transfer between $|a\rangle$ and $|b\rangle$. $|0\rangle$ or $|g\rangle$ represent the ground state of the system. (d) Schematic depiction and energy level scheme of the duplex with unstacked rBAM2 monomer with $|S_0\rangle$ denoting the ground state, $|S_1\rangle$ the first and $|S_2\rangle$ the second excited state. (e) Transient absorption map of rBAM2-D2 corresponding to the pure fifth-order signal.

To further analyze the dynamics associated with the excitonic manifold of the chromophores in rBAM2-D2, we used our technique of separating single- and multi-exciton dynamics in transient absorption (TA) spectroscopy by means of systematic intensity variation of the pump pulse.[17] The technique for separating single- and multi-exciton dynamics makes use of the perturbative formulation of nonlinear response and the measurement of pump–probe spectra at specific pump intensities to disentangle signal pathways corresponding to different orders of nonlinearity. Malý *et al.*[17] have developed a method to separately filter out the pure, i.e., contamination-free, third-order signal along with other pure higher-order signals. This enables one to study unexplored photophysical pathways associated with higher-order signals within the framework of ultrafast TA spectroscopy. Here we excited rBAM2-D2 by pumping the position of the excitonic band known from linear absorption measurements along with the monomeric shoulder (Fig. 3a). The corresponding signal response was collected by probing the system at a delay (*T*) after the pump pulse. The measurements were done at pump energies of 15 nJ, 45 nJ, and 60 nJ, based on the procedure described by Malý and co-workers (see SI, section 4.4, Fig. S4 for the pump-power dependence).[17] The probe-chirp-corrected transient map corresponding to the pure third-order response (Fig. 3b) shows a strong negative band at 515 nm and a weaker negative feature at 570 nm. The spectral positions of these two features match the two peaks in the linear absorption spectrum and the signal evolution over the delay *T* contains information about the dynamics of the corresponding single-exciton state, which we label $|a\rangle$, and the monomeric band $|S_1\rangle$, respectively (Figs. 3c, 3d). Since $|b\rangle$ is optically dark due to the H-type coupling arrangement, no corresponding transient could be observed. A strong positive broad band around 400–450 nm indicates excited-state absorption into higher excited states.

We also extract the pure fifth-order transient map (Fig. 3e). This fifth-order signal contains information about the biexciton state $|ab\rangle$ and higher excited states $|c_1\rangle$ and $|c_2\rangle$ constituting the manifold of doubly excited states. The energy of the biexciton state is given by the sum of the two single-exciton states in a Frenkel excitonic system, neglecting additional binding energy. A TA measurement carried out on rBAM2^{free} confirms that the higher-excited states $|c_1\rangle$ and $|c_2\rangle$ originate from the individual molecules and these states are energetically higher than the biexciton state $|ab\rangle$. This is because the broad excited-state absorption band in the dimer complex which is also observed in case of the free monomer is far blue-shifted with respect to the bleach signal of the single-exciton band (SI, Fig. S5). Global analysis on the third-order TA data of rBAM2-D2 and rBAM2^{free} indicates lifetimes of ~52 ps and ~164 ps, respectively (SI, Fig. S6). The 1.7 ns time constant of rBAM2-D2 observed by TCSPC originates from imperfectly stacked chromophores, which is also in agreement with the temperature-dependent steady-state emission of rBAM2-D2 (SI, Fig. S2d), resulting in a change of only the emission intensity and not the spectral shape. The strongly coupled dimer system rBAM2-D2 has a more efficient sandwich-type orientation between the chromophores compared to the shorter rBAM.[16] The orientation of the two dipoles and the degree of free rotation within each chromophore are two important factors that determine the radiative nature of rBAM dimers. While the

latter is the reason behind the increase in fluorescence quantum yield upon dimerization in rBAM,[16] the reduction in fluorescence in rBAM2-D2 can be rationalized by near perfect H-type aggregation.

The information about the exciton–exciton annihilation (EEA) dynamics of rBAM2-D2 is encompassed in the fifth-order transient map (Fig. 3e). In essence, the fifth-order signal can be described by numerous signal pathways which are depicted using energy ladder diagrams (SI, Fig. S7). The integrated signal contains contributions from ground-state-bleach-like pathways and the biexciton pathways, while all other contributions vanish for a perfect H-type homodimer.[23] Previously, it has been shown that the integrated fifth-order signal can be used to determine exciton diffusion in the material.[5,24] In the present case, we extract a transient at the maximum signal of rBAM2-D2 and avoid signal integration to exclude contributions from the rBAM2 monomer. The obtained fifth-order transient shows an immediate decay at early *T*, which can be attributed to both EEA and ultrafast transfer between the single-exciton states.[23] Ultrafast EEA can be rationalized by the close spatial vicinity of the two merocyanines within the RNA duplex, leading to no significant exciton diffusion before EEA because the excitons already overlap. The fast kinetics occur on a time scale which is in the order of the temporal resolution of our setup (60 fs). Similarly fast dynamics have also been reported in covalently linked squaraine dimers and trimers.[17,24,25] After EEA, only one exciton remains, which is reflected by the signal decay with the single-exciton lifetime (SI, Fig. S8).

In conclusion, we describe the synthesis and incorporation of the elongated merocyanine ribonucleotide rBAM2 into RNA oligonucleotides. rBAM2-labeled RNA strands show strongly enhanced fluorescence emission compared to the free chromophore, and a ca. 100 nm longer wavelength than previously reported BAM. In an RNA duplex containing two opposite rBAM2, dipolar stacking induced the formation of a non-fluorescent H-type aggregate. TCSPC revealed residual fluorescence of unstacked rBAM2 while the single- and multi-exciton dynamics of the stacked dimer were studied by ultrafast transient absorption spectroscopy including nonlinear order extraction. The fifth-order transient suggests that the proximity of the rBAM2 units in the RNA duplex leads to almost immediate exciton–exciton annihilation. Our work provides a motivation for the construction and analysis of more elaborate multi-chromophore assemblies including oligonucleotide scaffolds necessary for precise organization of multichromophoric systems to study fundamental processes of exciton transport.

This work was supported by the University of Würzburg and the Deutsche Forschungsgemeinschaft (DFG, German Research Foundation) grant no. 423942615 to T.B. We thank Julian Fichtner and Frank Würthner for access to the TCSPC setup and stimulating discussions. We thank Rebecca Fröhlich for assistance with the TA setup.

Conflicts of interest

There are no conflicts of interest to declare.

Notes and references

1. Y. Hong, J. Kim, W. Kim, C. Kaufmann, H. Kim, F. Würthner and D. Kim, *J. Am. Chem. Soc.*, 2020, **142**, 7845-7857.
2. O. A. Sytina, I. H. M. van Stokkum, R. van Grondelle and M. L. Groot, *J. Phys. Chem. A*, 2011, **115**, 3936-3946.
3. Y. Hong, M. Rudolf, M. Kim, J. Kim, T. Schembri, A.-M. Krause, K. Shoyama, D. Bialas, M. I. S. Röhr, T. Joo, H. Kim, D. Kim and F. Würthner, *Nat. Commun.*, 2022, **13**.
4. A. Aster, F. Zinna, C. Rumble, J. Lacour and E. Vauthey, *J. Am. Chem. Soc.*, 2021, **143**, 2361-2371.
5. P. Malý, J. Lüttig, A. Turkin, J. Dostál, C. Lambert and T. Brixner, *Chem. Sci.*, 2020, **11**, 456-466.
6. H. Kashida, K. Sano, Y. Hara and H. Asanuma, *Bioconjugate Chem.*, 2009, **20**, 258-265.
7. P. Cunningham, Y. C. Kim, S. A. Díaz, S. Buckhout-White, D. Mathur, I. L. Medintz and J. S. Melinger, *J. Phys. Chem. B*, 2018, **122**, 5020-5029.
8. O. A. Mass, C. K. Wilson, S. K. Roy, M. S. Barclay, L. K. Patten, E. A. Terpetschnig, J. Lee, R. D. Pensack, B. Yurke and W. B. Knowlton, *J. Chem. Phys. B*, 2020, **124**, 9636-9647.
9. N. A. Pace, S. P. Hennelly and P. M. Goodwin, *J. Phys. Chem. Lett.*, 2021, **12**, 8963-8971.
10. L. I. Markova, V. L. Malinovskii, L. D. Patsenker and R. Häner, *Org. Biomol. Chem.*, 2012, **10**, 8944-8947.
11. D. Baumstark and H.-A. Wagenknecht, *Angew. Chem. Int. Ed.*, 2008, **47**, 2612-2614.
12. L.-A. Fendt, I. Bouamaied, S. Thöni, N. Amiot and E. Stulz, *J. Am. Chem. Soc.*, 2007, **129**, 15319-15329.
13. S. M. Hart, J. L. Banal, M. A. Castellanos, L. Markova, Y. Vyborna, J. Gorman, R. Häner, A. P. Willard, M. Bathe and G. S. Schlau-Cohen, *Chem. Sci.*, 2022, **13**, 13020-13031.
14. S. M. Hart, W. J. Chen, J. L. Banal, W. P. Bricker, A. Dodin, L. Markova, Y. Vyborna, A. P. Willard, R. Häner, M. Bathe and G. S. Schlau-Cohen, *Chem*, 2021, **7**, 752-773.
15. S. M. Hart, X. Wang, J. Guo, M. Bathe and G. S. Schlau-Cohen, *J. Phys. Chem. Lett.*, 2022, **13**, 1863-1871.
16. J. Dietzsch, D. Bialas, J. Bandorf, F. Würthner and C. Höbartner, *Angew. Chem. Int. Ed.*, 2022, **61**, e202116783.
17. P. Malý, J. Lüttig, P. A. Rose, C. Lambert, J. J. Krich and T. Brixner, *Nature*, 2023, **616**, 280-287.
18. R. L. Simmons, R. T. Yu and A. G. Myers, *J. Am. Chem. Soc.*, 2011, **133**, 15870-15873.
19. T. E. Kodger, P. J. Lu, G. R. Wiseman and D. A. Weitz, *Langmuir*, 2017, **33**, 6382-6389.
20. L. A. Ernst, R. K. Gupta, R. B. Mujumdar and A. S. Waggoner, *Cytometry*, 1989, **10**, 3-10.
21. G. E. Plum, *Curr. Protoc. Nucleic Acid Chem.*, 2000, 7.3.1-7.3.17.
22. U. Rösch, S. Yao, R. Wortmann and F. Würthner, *Angew. Chem. Int. Ed.*, 2006, **45**, 7026-7030.
23. C. Heshmatpour, P. Malevich, F. Plasser, M. Menger, C. Lambert, F. Sanda and J. Hauer, *J Phys Chem Lett*, 2020, **11**, 7776-7781.
24. P. Malý, S. Mueller, J. Lüttig, C. Lambert and T. Brixner, *J. Chem. Phys.*, 2020, **153**, 144204.
25. C. Heshmatpour, P. Malevich, F. Plasser, M. Menger, C. Lambert, F. Šanda and J. Hauer, *J. Phys. Chem. Lett.*, 2020, **11**, 7776-7781.

